Comparison of the thermal decomposition processes of several aminoalcohol-based ZnO inks with one containing ethanolamine

Alberto Gómez-Núñez[1], Pere Roura[2], Concepción López[3], Anna Vilà[1*]

[1]University of Barcelona, Department of Electronics, Martí i Franquès 1, E08028-Barcelona, Spain.

[2]University of Girona, Department of Physics, Campus Montilivi, Edif. PII, E17071-Girona, Catalonia, Spain.

[3]University of Barcelona, Department of Inorganic Chemistry, Martí i Franquès 1, E08028-Barcelona, Spain.

*Corresponding author: Phone: +34934039170, Fax: +34934021148, avila@el.ub.edu, anna.vila@ub.edu

Abstract

Four inks for the production of ZnO semiconducting films have been prepared with zinc acetate dihydrate as precursor salt and one among the following aminoalcohols: aminopropanol (APr), aminomethyl butanol (AMB), aminophenol (APh) and aminobenzyl alcohol (AB) as stabilizing agent. Their thermal decomposition process has been analyzed in situ by thermogravimetric analysis (TGA), differential scanning calorimetry (DSC) and evolved gas analysis (EGA), whereas the solid product has been analysed ex-situ by X-ray diffraction (XRD) and infrared spectroscopy (IR). Although, except for the APh ink, crystalline ZnO is already obtained at 300 ºC, the films contain an organic residue that evolves at higher temperature in the form of a large variety of nitrogen-containing cyclic compounds. The results indicate that APr can be a better stabilizing agent than ethanolamine (EA). It gives larger ZnO crystal sizes with similar carbon content. However, a common drawback of all the amino stabilizers (EA included) is that nitrogen atoms have not been completely removed from the ZnO film at the highest temperature of our experiments (600 ºC).

INTRODUCTION

ZnO is widely used as n-type semiconducting material because of its low cost combined with excellent electronic properties. It can be easily nanostructured [1-5] using scalable processing methods based on chemical routes, such as sol-gel [6]. However, stabilization of the metal organic precursors in solvents is one of the main problems in printed electronics [7,8]. Consequently, stabilizers must be added but their effect on the final ZnO structure is not negligible. It has been found that thiols limit the growth of ZnO nanoparticles [9,10] and stabilizers lead to different film morphologies [11]. Furthermore, orientation of ZnO crystals strongly depends on the particular stabilizer [12].

Ethanolamine is one of the best stabilizers that are used to prepare ZnO for thin-film devices from inks based on zinc acetate salts. It leads to high mobility and low dark current values [13]. Nevertheless, we have recently shown that, after thermal treatment up to 600 ºC, films obtained from Zn acetate are contaminated by nitrogen atoms coming from the amine group [14]. The aim of this paper is to examine the possibility to substitute ethanolamine by other aminoalcohols to get a cleaner final ZnO film. It has been argued that the molecule flexibility must have strong influence on bond torsion and breaking, and then onto the thermal decomposition process of the precursor film [15]. So, we have analysed several aminoalcohols (Fig.1) with different molecular rigidity to assess if they behave better than ethanolamine.
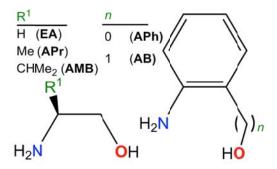

Figure 1. Molecular structure of the aliphatic (left) and aromatic (right) aminoalcohols used in this study.

EXPERIMENTAL PROCEDURE

Samples preparation

Zinc acetate dihydrate [$Zn(CH_3COO)_2 \cdot 2H_2O$, **ZAD**] was purchased from Panreac, 2-metoxyethanol (**ME**) from Aldrich, ethanolamine (**EA**) from Acrös Organics and the other aminoalcohols [(S)-(+)-2-amino-1-propanol (**APr**), (S)-(+)-2-amino-3-methyl-1-butanol (**AMB**), 2-aminophenol (**APh**) and 2-aminobenzyl alcohol (**AB)**] from Aldrich. All the reagents were used as received. Figure 1 shows the molecular structure of EA and the other closely related aminoalcohols used in this study.

The inks were prepared as follows. 0.5 g of ZAD (2.3 mmol) were treated with an equimolar amount of the corresponding stabilizer (EA, APr, AMB, APh or AB) and mixed in 5 mL of solvent (ME). All mixtures were kept at 60 ºC under continuous stirring for 30 min. Except for the inks containing aromatic stabilizers (APh and AB), that became dark due to their strong photoreactivity, the other ones remained transparent clear solutions for weeks.

Precursor thin films were deposited by drop coating on glass substrates.

Thermal analysis

To study the thermal evolution of the inks, thermogravimetric (TGA), and differential scanning calorimetry (DSC) analyses were done in dry air and pure oxygen atmospheres (flow rate of 50 mL/min) at a heating rate of 10 ºC/min up to 600 ºC in uncovered alumina and aluminium pans, respectively. A drop of ink corresponding to a ZnO mass around 200 µg was poured inside the pans. The ink wetted the inner walls of the pan leaving behind a film of "nominal thickness" (i.e. the thickness of ZnO, if it were a dense homogeneous film) around 0.5 µm. We used the TGA-851e and DSC-822e apparatus of Mettler-Toledo.

Complementary Evolved Gas Analysis (EGA) of the evolved species during ink decomposition was done in vacuum at 20 ºC/min up to 600 ºC, using a MKS quadrupole mass spectrometer (Microvision Plus).

Structural analyses

The films structure was analysed after heating them at 10 ºC/min in air up to 300 and 600 ºC. The first samples were kept for 5 min at 300 ºC, whereas the second ones were cooled down without any delay after reaching 600 ºC. X-ray diffraction (XRD) measurements were carried out with a PANalytical X'Pert PRO MPD Alpha1 powder diffractometer in

Bragg-Brentano $\theta/2\theta$ geometry with Cu Kα_1 radiation (λ = 1.5406 Å). Films were scratched from the substrate and the resulting powder was put inside KBr pellets for infrared (IR) spectroscopy with a Nicolet 400FTIR instrument. Carbon and nitrogen content was quantified by elemental organic analyses (EOA) with the Thermo EA Flash 2000 (Thermo Scientific, Milan, Italy) equipment working in standard conditions (helium flow: 140 ml/min; combustion furnace at 950 ºC; chromatographic column oven at 65 ºC). And, finally, film morphology was observed by scanning electron microscopy (SEM) with a JEOL JSM-7100F and a JEOL J-6510 in planar and cross-section views.

RESULTS AND DISCUSSION

TG/DSC experiments

After solvent evaporation, that finishes below 150 ºC (ME boiling point, 124 ºC), thermal decomposition of the inks is revealed by two mass-loss steps (Fig.2). According to previous observations on the EA ink [14], ZnO appears after the first decomposition step with maximum decomposition rate in the 230-270 ºC range depending on the particular stabilizer. DSC experiments indicate that the first decomposition step is endothermic (in the case of EA and APr) or isenthalpic (for APh and AB) and, when exothermic in air (as in the case of AMB – Fig.2a), the decomposition temperature remains the same as in pure oxygen. This observation shows that a higher oxygen concentration does not advance the decomposition reaction; i.e. this step is not triggered by reaction with the oxygen molecules of the furnace atmosphere.

The second mass-loss step that corresponds to elimination of the organic residue is much more dependent on the particular stabilizer. It is centred on around 270 ºC for the aliphatic stabilizers (Fig.2a) whereas it appears at higher temperature for the APh (440 ºC) and AB (480 ºC) inks (Fig.2b). Furthermore, the inks with aromatic stabilizers lose much more mass during the second step (Fig.2b), as expected because of the large mass and high thermal stability of the aromatic ring. Elimination of the organic residue proceeds through reaction with oxygen leading to prominent exothermic DSC peaks (Fig.2), the decomposition heat being higher for the aromatic stabilizers.

It must be pointed out that the second mass-loss step is not related with evaporation of the stabilizer. Firstly, because its temperature is not correlated with the stabilizer boiling point (300 ºC for APh and 160 ºC for AB). Secondly, because during ink formation the

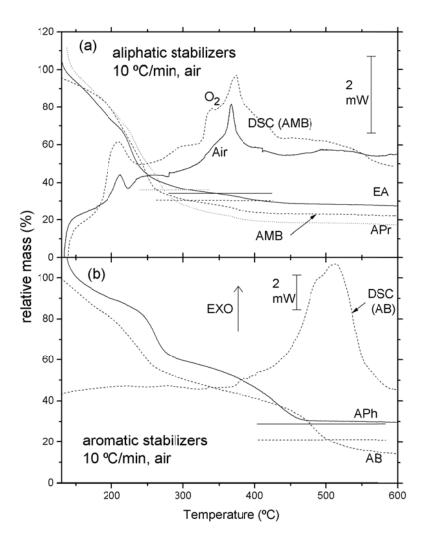stabilizer probably reacts with ZAD to form a complex precursor molecule, as shown for EA [14].

Figure 2. TG and DSC curves of ink decomposition for: a) aliphatic and b) aromatic stabilizers. TG curves are normalized to the mass after solvent evaporation. Horizontal lines are the expected final masses if the residue is 100% ZnO.

Finally, it is worth noting that, except for the APh TG curve, the recorded mass at 600 ºC is smaller than the expected mass for pure ZnO (horizontal lines in Fig.2). In other words, Zn atoms have been lost during the decomposition process (presumably during the first step). This phenomenon has already been reported for ZAD [16] and for CuO metal organic precursors [17]. The Zn loss has been accurately quantified for the EA ink by measuring the mass of the residue outside the TG furnace with an independent more stable microbalance,

5

and comparing this mass with the one obtained after repeating the experiment with the ink spread on a glass substrate. The TG curves normalized to the final mass are shown in Fig.3. The horizontal line marks the mass of ZAD+EA precursor if Zn were not lost. Although we cannot discard that some ME evaporation still occurs up to 150 ºC, comparison of this level with the experimental TG curves suggests that more than 25% of Zn is lost during decomposition. This experiment is also useful to assess that the TG experiments done with alumina pans (those of Fig.2) reproduce reasonably well what occurs in films. Anyway, since, as said above, oxygen does not trigger decomposition, the observed shift by 20 ºC in the first decomposition step can be attributed to a surface effect, i.e. an easier transport of volatiles out of films that out of bulk material [17].
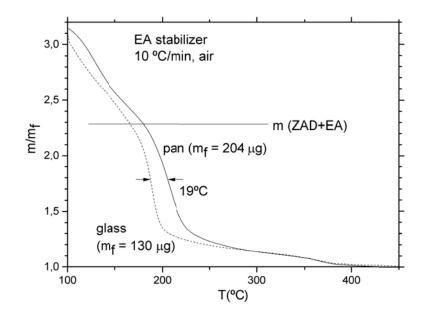

Figure 3. TG curves of the EA ink decomposed inside an alumina pan and on a glass substrate. Mass is normalized to the final mass measured externally to the TG apparatus. Horizontal line: mass of the ZAD+DEA precursor if no Zn atoms were lost.

XRD, IR and EOA results

ZnO formation after the first mass-loss step has been assessed by XRD (Fig. 4). Except for APh that, after the second step, degraded becoming a powder and consequently will not be included in the studies for 600 ºC presented in the following sections, after heating up to 300 ºC all the inks exhibit the characteristic peaks of hexagonal ZnO sometimes with

(002) preferential orientation (Fig.4a). In the AB curve, one additional peak of unknown origin (nor does it correspond to the ZnO cubic phase) is observed. All peaks are very broad. Application of Scherrer's formula delivers crystal size values ranging between 7 and 13 nm; these extreme values are for EA and for AB films, respectively. This poor crystalline quality is partially due to the large content of organic residue revealed by IR spectroscopy.
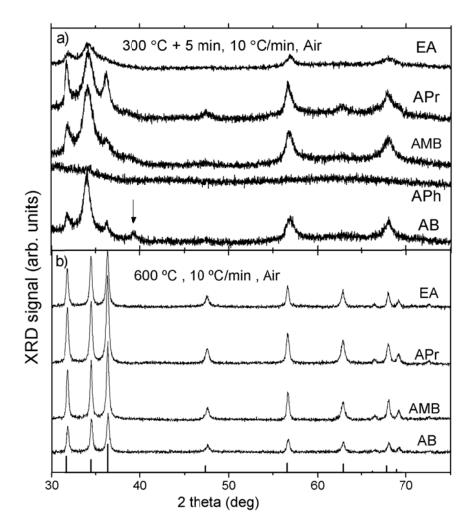

Figure 4. XRD spectra measured after heating the films up to 300ºC (a) and 600ºC (b) (the APh film did not survive at this temperature). At the bottom of figure b, the bars are the pattern of pure ZnO (JCPDS 36-1451). The arrow in a) indicates the peak of an unknown phase.

IR spectra are consistent with XRD results in the sense that all films, except the APh film, have the characteristic vibrational band of ZnO at 400-600 cm^{-1} [18] already at 300 ºC (Fig.5a). The absence of this band for the APh film means that ZnO has not been produced

after the first decomposition step. In addition, all IR spectra contain very intense carboxylate bands centred at 1580 and 1410 cm^{-1} [19]. Again, retardation of APh film decomposition is confirmed by the bands at 1500 (weak) and 1280 (intense) cm^{-1} related to the precursor [20].
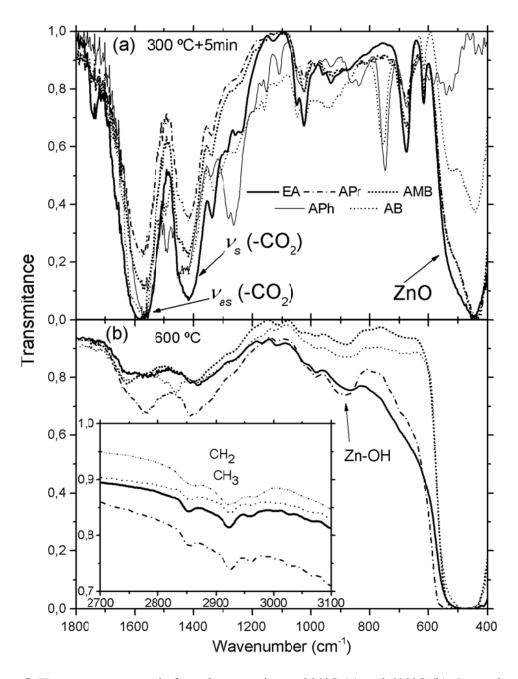

Figure 5. IR spectra measured after a heat treating at 300ºC (a) and 600ºC (b). Inset: detail of the bands related to CH_3 and CH_2 groups.

The organic residue contribution to the IR spectra is substantially reduced after the heat treatment at 600 ºC (Fig.5b). Now, the absorbance due to ZnO reaches saturation (zero

transmittance) for all films. Unfortunately, the method used to make these measurements (film flakes inside KBr pellets) precludes any attempt of quantification. Consequently, although one can see varying intensities of the carboxylate and (aliphatic) C-H-stretching bonds [21] (inset of Fig.5b) from film to film, from these slight differences one cannot infer higher or lower organic content. Instead, the elemental C and N contents have been quantified by EOA. The determined percentage of N is below the technique sensitivity (0.2%), but quantification of C has been possible (see Table I). EA and APr films have the lowest carbon content (0.2-0.3%) and the AB film, the highest (3.5%).

Removal of the organic residue as well as thermal activation of grain growth improves considerably the film crystalline quality at 600 ºC. XRD peaks are much narrower and attributable to wurtzite ZnO (Fig.4b). The AB and APr films have the largest crystal sizes (27-28 nm) whereas the smallest ones are found in the AMB and EA films (21 nm) (Table I). The lack of any significant preferential crystalline orientation can be due to the use of low-boiling temperature solvent [6]. However, use of adequate substrates (Pt(111) and amorphous SiN_x on c-Si) can promote preferential orientation along the c-axis even for ZAD+EA inks dissolved in ME [12].

Table I. Average ZnO crystal size at 600 ºC obtained from the XRD curves by applying Scherrer's formula to the (100), (002) and (101) peaks; and carbon content measured by elemental analysis at the same temperature.

	EA	APr	AMB	AB
crystal size (nm)	21.1	26.8	21.2	28.0
C content (%)	0.2-0.3	0.2-0.3	0.4	3.5

Analysis of the evolved gases

EGA experiments in vacuum have allowed detecting the volatile products of the inks decomposition. Many fragments have been detected up to m/z=150 whose identification has been based on the computational and experimental work of Bouchoux's group on the reactivity of aliphatic aminoalcohols [22]. These authors found that their dissociation produces a number of nitrogenated cyclic fragments, the simplest ones being azidine (m/z=44), azetidine (58), pyrolidine (68) and piperidine (85). In Fig.6a we have plotted the EGA curves of several intense signals that can be assigned to these cyclic fragments during decomposition of the AMB ink. These curves can be compared with the mass-loss curve

(dTGA curve) of Fig.6b. Notice that, whereas some cycles (m/z=127 and 85) evolve during the first decomposition step (the first dTGA intense peak) or up to the second decomposition step (the smallest peak at 380 ºC), two cycles (m/z=44 and 68) still evolve at the highest temperature of the experiment. Consequently, the EGA results constitute a proof that nitrogen still remains as an impurity after the usual maximum temperature (600 ºC) of ZnO film synthesis from ZAD inks. This conclusion can be extended to all the inks studied here. In Fig.7, we summarize the nitrogenated cyclic fragments detected for the other inks and their evolution.
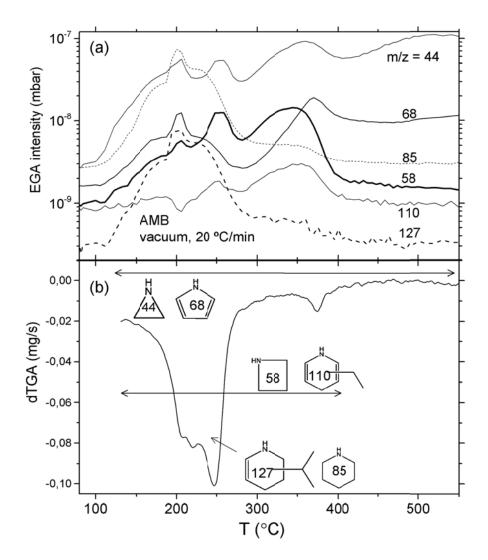

Figure 6. a) EGA curves of intense volatile fragments detected during decomposition of the AMB ink in vacuum. b) Mass-loss rate curve during decomposition of AMB, drawn to indicate the temperature range in which main volatiles are detected.
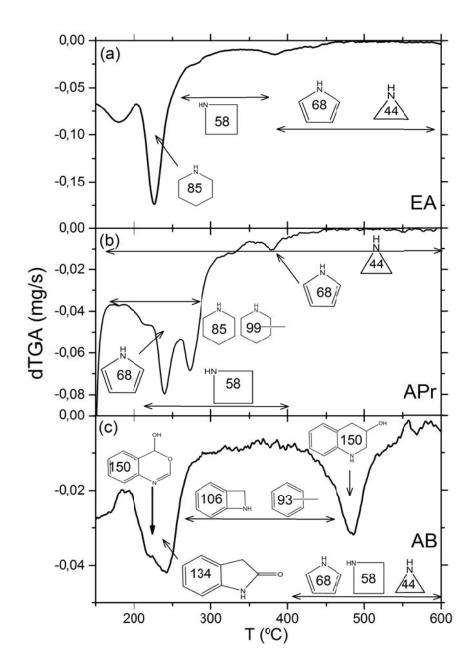
Figure 7. Approximated temperature range in which nitrogenated cyclic fragments are detected by EGA during decomposition of the EA (a), APr (b) and AB (c) inks.

Film morphology

Finally, the films surface morphology has been observed in plane-view by SEM (Fig.8). With the exception of the APh one, all inks have led to continuous ZnO films without cracks. However, films are far from flat and exhibit pronounced ripples giving rise to characteristic patterns similar to those already reported for ZnO [23] and for other oxide films [24]. They probably arise during the first decomposition step. Since precursor decomposition

results in a drastic reduction of its volume whereas the substrate hinders any in-plane contraction, stress arises in the film. Ripples are a mean to relieve this stress [24]. In fact, ripples and cracks are defects that make difficult to obtain high-quality thick films by chemical-solution routes. Among our films, AMB leads to the flattest surface whereas, with EA, ripples are the most pronounced.
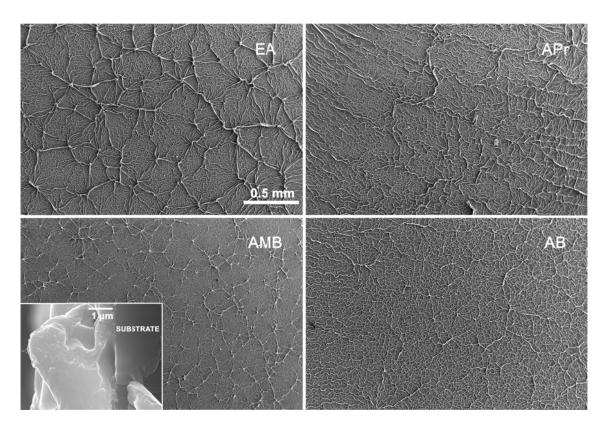

Figure 8. SEM micrographs of the films treated at 600ºC. Inset: cross section of the AMB film.

CONCLUSIONS

ZnO films have been prepared from inks containing Zn acetate dihydrate and several aminoalcohols. Concerning thermal decomposition, the aliphatic stabilizers (EA, APr and AMB) behave similarly with a main decomposition step around 250 ºC followed by a minor mass-loss step at 370 ºC. This is in contrast with the aromatic stabilizers (APh and AB), that experience an important mass-loss step above 400 ºC. Although crystalline ZnO can be found already at 300 ºC, crystal quality is poor unless films are heated up to 600 ºC to reduce the organic residue and promote crystal growth. Compared with EA, ZnO crystallites are larger

for the AB and APr inks and of similar size with AMB. In contrast, APh degrades to powder. Carbon contamination quantified by EOA reaches a minimum concentration with EA and APr, while for AB it is 10 times higher. Contamination by nitrogen could not be quantified. However, analysis of the evolved gases indicates that nitrogen atoms have not been completely removed at 600 ºC. Films are not homogeneous; all of them have ripples that arise from internal stresses during decomposition.

To sum up, the comparative studies undertaken for the 5 aminoalcohols proposed as stabilizers in ink manufacture and their evolution to ZnO films demonstrate the influence and effect of the linkers (spacers of the aminoalcohol on the global process). We have proved that: a) aromatic aminoalcohols behave worse than EA due to either their degradation and transformation to powdered material (APh) or the retention of higher contents of carbon after the thermal treatment; b) aliphatic aminoalcohols are clearly a better choice, giving ZnO films with less doping carbon but showing ripples whose height decreases as follows EA > APr > AMB. These aminoalcohols $H_2N-CH(R^1)CH_2OH$ only differ in the nature and bulk of the substituent R' that could play a key role in determining the morphology and also the crystal sizes of the films.

REFERENCES

[1] C.C. Lin, Y.Y. Li, Synthesis of ZnO nanowires by thermal decomposition of zinc acetate dihydrate, Mat. Chem. Phys., 113(1) (2009), 334–337.

[2] X. Su, Z. Zhang, Y. Wang, M. Zhu, Synthesis and photoluminescence of aligned ZnO nanorods by thermal decomposition of zinc acetate at a substrate temperature of ~250 ºC. J. Phys. D, 38(21) (2005) 3934–3937.

[3] A. Tarat, R. Majithia, R. Brown, M.W. Penny, K.E. Meissner, T.G.G. Maffeis, Synthesis of nanocrystalline ZnO nanobelts via pyrolytic decomposition of zinc acetate nanobelts and their gas sensing behavior. Surf. Sci., 606(7-8) (2012) 715–721.

[4] R.S. Wang, P.J. Thomas, P. O'Brien, Nanocrystalline ZnO with ultraviolet luminescence. J. Phys. Chem. B, 110(9) (2006) 4099–104.

[5] Y. Yang, H. Chen, B. Zhao, X. Bao, Size control of ZnO nanoparticles via thermal decomposition of zinc acetate coated on organic additives. J. Cryst. Growth, 263(1-4) (2004) 447–453.

[6] L. Znaidi, Sol-gel-deposited ZnO thin films: A review. Mat. Sci. Eng. B, 174(1-3) (2010) 18–30.

[7] F. Boudjouan, A. Chelouche, T. Touam, D. Djouadi, S. Khodja, M. Tazerout, Z. Hadjoub, Effects of stabilizer ratio on photoluminescence properties of sol-gel ZnO nano-structured thin films. J. Luminescence, 158 (2015) 32–37.

[8] S. Khodja, T. Touam, A. Chelouche, F. Boudjouan, D. Djouadi, Z. Hadjoub, A. Boudrioua, Effects of stabilizer ratio on structural, morphological, optical and waveguide properties of ZnO nano-structured thin films by a sol–gel process. Superlattices and Microstructures, 75 (2014) 485–495.

[9] A.K. Singh, V. Viswanath, V.C. Janu, Synthesis, effect of capping agents, structural, optical and photoluminescence properties of ZnO nanoparticles, J. Luminescence, 129 (2009) 874-878.

[10] E.M. Wong, P.G. Hoertz, C.J. Liang, B.M. Shi, G.J. Meyer, P.C. Searson, Influence of organic capping ligands on the growth kinetics of ZnO nanoparticles, Langmuir, 17 (2001) 8362-8367.

[11] K. Govender, D.S. Boyle, P.B. Kenway, P. O'Brien, Understanding the factors that govern the deposition and morphology of thin films of ZnO from aqueous solution, J. Mat. Chem., 14 (2004) 2575-2591.

[12] S.H. Yoon, D. Liu, D. Shen, M. Park, D.J. Kim, Effect of chelating agents on the preferred orientation of ZnO films by sol-gel process, J. Mat. Sci., 43 (2008) 6177-6181.

[13] A.H. Adl, P. Kar. S. Farsinezhad, H. Sharma, K. Shankar, Effect of Sol Stabilizer on the Structure and Electronic Properties of Solution-Processed ZnO thin Films, RSC Adv., 5 (2015) 87007 - 87018.

[14] A. Gómez-Núñez, C. López, S. Alonso-Gil, P. Roura, A. Vilà, Study of a sol–gel precursor and its evolution towards ZnO. Mat. Chem. Phys., 162 (2015) 645-651.

[15] P.H. Vajargah, H. Abdizadeh, R. Ebrahimifard, M.R. Golobostanfard, Sol-gel derived ZnO thin films: Effect of amino-additives. App. Surf. Sci., 285P (2013) 732–743.

[16] T. Arii, A. Kishi, The effect of humidity on thermal process of zinc acetate. Thermochim. Acta. 400 (2003) 175–185.

[17] P. Roura, J. Farjas, H. Eloussifi, L. Carreras, S. Ricart, T. Puig, X. Obradors, Thermal analysis of metal organic precursors for functional oxide preparation: Thin films versus powders. Thermochim. Acta. 601 (2015) 1-8.

[18] H. He, F. Zhuge, Z. Ye, L. Zhu, B. Zhao, J. Huang, Defect-related vibrational and photoluminescence spectroscopy of a codoped ZnO : Al : N film. J. Phys. D, 39 (2006) 2339-2342.

[19] K. Nakamoto, Infrared and Raman Spectra of Inorganic and Coordination Compounds, 5th ed., Wiley, (1997). New York, USA.

[20] W.P. Grifith, T.Y. Koh, Vibrational spectra of 1,2-benzenedithiol, 2-aminothiophenol and 2-aminophenol and their SER spectra, Spectrochim. Acta A, 51(2) (1995) 253–260.

[21] A. Kołodziejczak-Radzimska, E. Markiewicz, T. Jesionowski, Structural Characterisation of ZnO Particles Obtained by the Emulsion Precipitation Method. J. Nanomat. (2012), Article ID 656353, 9 p.

[22] G. Bouchoux, N. Choret, F. Berruyer-Penaud, R. Flammang, Thermochemistry and unimolecular reactivity of protonated α,ω-aminoalcohols in the gas phase. Int. J. Mass Spectrom., 217(1-3) (2002) 195–230.

[23] N.V. Kaneva, G.G. Yordanov, C.D. Dushkin, Manufacturing of patterned ZnO films with application for photoinitiated decolorization of malachite green in aqueous solutions, Bull.Mater.Sci. 33 (2010) 111-117.

[24] K. Zalamova, N. Roma, A. Pomar, S. Morlens, T. Puig, J. Gázquez, A.E. Carrillo, F. Sandiumenge, S. Ricart, N. Mestres, X. Obradors, Smooth stress relief of trifluoroacetate metal-organic solutions for $YBa_2Cu_3O_7$ film growth, Chem.Mater. 18 (2006) 5897-5906.